# Taylor coefficients of the thermodynamic potential to sixth order in the vector interaction extended NJL model

**Taylor-Koeffizienten des thermodynamischen Potenzials bis zur sechsten Ordnung im mit Vektor-Wechselwirkung erweiterten NJL-Modell**

Bachelor-Thesis von Stephen Frieß aus Miltenberg

September 2013

TECHNISCHE UNIVERSITÄT DARMSTADT

Fachbereich Physik
AG Nuclei, Hadrons and Quarks
Institut für Kernphysik

Taylor coefficients of the thermodynamic potential to sixth order in the vector interaction extended NJL model
Taylor-Koeffizienten des thermodynamischen Potenzials bis zur sechsten Ordnung im mit Vektor-Wechselwirkung erweiterten NJL-Modell

Vorgelegte Bachelor-Thesis von Stephen Frieß aus Miltenberg

1. Gutachten: PD Dr. Michael Buballa
2. Gutachten: Prof. Dr. Jochen Wambach

Tag der Einreichung:

**Erklärung zur Bachelor-Thesis**

Hiermit versichere ich, die vorliegende Bachelor-Thesis ohne Hilfe Dritter nur mit den angegebenen Quellen und Hilfsmitteln angefertigt zu haben. Alle Stellen, die aus Quellen entnommen wurden, sind als solche kenntlich gemacht. Diese Arbeit hat in gleicher oder ähnlicher Form noch keiner Prüfungsbehörde vorgelegen.

Darmstadt, den 27.09.13

(Stephen Frieß)

**Abstract**

In analogy to the Taylor expansion technique which extends lattice QCD calculations from $\mu = 0$ to $\mu < T$, we will calculate the Taylor coefficients of the thermodynamic potential $\Omega$ up to sixth order in the expansion point $\mu/T = 0$ using an extended NJL model. In particular the NJL model is extended by a vector interaction term which comes with a coupling strength $G_V$ as parameter. The coupling strength $G_V$ will be varied and the influence of it will be investigated. In comparison to lattice QCD results we will see that the high temperature limits as well as the course of the Taylor coefficients can best be replicated when completely neglecting the vector interaction channel in the NJL model (thus $G_V \equiv 0$).

## Contents

## 1 Introduction

Quantum Chromodynamics is the established quantum field theory describing the strong interaction between quarks and gluons. In attempts to describe the thermodynamics of the early universe and compact stars, one introduces the concept of QCD matter. In QCD matter, quarks and gluons are the essential degrees of freedom. First principle calculations of QCD thermodynamics cannot be done analytically, thus one developed the numerical technique of lattice QCD. However a major flaw of the lattice QCD approach is that it cannot be directly extended to $\mu \neq 0$ due to the fermion sign problem [1]. To get some approximate knowledge about the QCD thermodynamics on the $T$-$\mu$ plane by theoretical studies, one developed various methods [1, 2] which have some reliability for the vicinity of $\mu < T$. One of these methods is to perform a Taylor expansion of observables in terms of $\mu/T$ and neglect higher orders at will.

A completely different approach to investigate the $T$-$\mu$ plane of QCD matter by theoretical studies, is to use field theories which are capable of replicating some prominent features of QCD. Such an approach is the Nambo-Jona-Lasinio model [3, 4]. The basis of the interpretation of the NJL model is mainly based upon the fact that the NJL-Lagrangian has its chiral symmetry in common with the QCD-Lagrangian [5]. The NJL model can be effectively used to describe various phase transitions and thermodynamic properties, which are thought to occur for QCD matter. Constructing the NJL-Lagrangian solely based upon symmetry considerations allows one to add various interaction terms. The basic NJL-Lagrangian as found in most papers is only based upon a scalar and pseudo-scalar interaction term grouped together by a coupling constant $G_S$.

In the following we will consider an extended NJL-Lagrangian with a vector interaction term. The natural question which is raised when one extends the NJL-Lagrangian, is whether or not these extensions yield better results in comparison to lattice QCD for the vicinity of $\mu < T$. In this study we will answer this question by analogously calculating Taylor coefficients up to sixth order in the NJL model and comparing them to results obtained in lattice QCD calculations [6, 7]. For this purpose we will vary the vector coupling strength $G_V$ and investigate the effects on the coefficients as well as various functions.

## 2 Theoretical foundations

In the following we will start with an introduction to Quantum Chromodynamics, explaining some of its fundamental properties and then discussing associated Lagrangians and symmetries. We will especially focus on the symmetries of the 2d flavour space. We then switch to a discussion of QCD matter on basis of the QCD phase diagram, explaining the internal structure of the phase diagram and the problems to properly investigate it. From this we will see the necessity of alternative approaches. Motivated by this, the NJL model as an alternative field theory will be introduced, which can be used to investigate the phase diagram. Basis for these results are, that a majority of the global symmetries in the NJL model are common with those discussed in the section about QCD. The discussion of the NJL model will then be completed with some details provided on how to harness the model for the later calculations.

### 2.1 Quantum Chromodynamics

*Quantum Chromodynamics* is the established quantum field theory describing the strong interaction between quarks and gluons. Its most important features are colour confinement and asymptotic freedom.

*Colour confinement* is the observed property that if one assigns colour charges red, green and blue as well as corresponding anti-colours to quarks and gluons, one will only find bound systems such that the net colour charge is always white. An important implication from colour confinement is that various coloured composite particles such as $qq$ or $\overline{q}qqq$, etc. are forbidden to exist, whereas colour neutral states such as mesons ($\overline{q}q$) and baryons ($qqq$) form bound states. Hypothetically colour confinement also allows the existence of objects such as glueballs and various multi-quark states like e.g. tetra-quarks such as the recently discovered possible candidate $\mathrm{Z}_C(3900)$ [8, 9].

*Asymptotic freedom* is the property that quarks and gluons behave like quasifree[1] particles for high energies and small distances. The notion of asymptotic freedom implies an energy dependent coupling strength $\alpha_s(E)$. In particular asymptotic freedom in QCD means $\lim_{E\to\infty}\alpha_s(E) = 0$ [10]. Historically it was first thought to be impossible to construct a quantum field theory which features asymptotic freedom, until Politzer, Gross and Wilczek proved in 1973 that non-abelian gauge theories (Yang-Mills theories) do indeed maintain asymptotic freedom.

The Lagrangian of Quantum Chromodynamics is given by [11]:

$$\mathscr{L}_{\mathrm{QCD}} = \sum_f \overline{q}_f (i\not{D} - m_f) q_f - \frac{1}{4} G^a_{\mu\nu} G^{\mu\nu}_a, \tag{2.1}$$

where $q_f$ is a quark wave function of flavour $f$, $\overline{q}_f = q_f^\dagger \gamma^0$, $\not{D}$ the gauge covariant derivative $D_\mu = \partial_\mu + igA_\mu$ in Feynman slash notation $\not{a} := \gamma^\mu a_\mu$ with coupling strength $g$ and gluon vector potentials $A_\mu$ and $G^a_{\mu\nu}$ gluon field strengths. We implicitly assume that the quark wave functions live in the Hilbert space $\mathscr{H} = \mathscr{H}_C \otimes \mathscr{H}_D \otimes \mathscr{H}_F$, which is a product of the Hilbert spaces for colour, Dirac and flavour wave function.

This Lagrangian has several symmetries. Gauge invariance of the local $\mathrm{SU}(3)_C$ group in colour space gives rise to the gluons. Maintaining this symmetry will forbid us to add any gluonic terms incorporating a mass [10]. Thus gluons are massless. Further important symmetries can be found in flavour space. In this case however we will have to restrict ourselves upon a given number of flavours. Since the scope of this work will focus on the study of a two flavour model incorporating the up and down quark, we will restrict ourselves upon these. However one can analogously study flavour space symmetries for more than two flavours. Further notes upon a three flavour model incorporating the strange quark can be found in Ref. [5]. To study symmetries we decompose Eq. (2.1) into the following form:

$$\mathscr{L}_{\mathrm{QCD}} = \mathscr{L}_{\mathrm{chiral}} - \sum_{f\in\{u,d\}} \overline{q}_f \underline{m} q_f + \mathscr{L}_{scbt}, \tag{2.2}$$

where we have introduced the mass matrix $\underline{m} = \mathrm{diag}(m_u, m_d)$ and the chiral Lagrangian into which we incorporated the gluon field strengths:

$$\mathscr{L}_{\mathrm{chiral}} = \sum_{f\in\{u,d\}} \overline{q}_f i\not{D} q_f - \frac{1}{4} G^a_{\mu\nu} G^{\mu\nu}_a. \tag{2.3}$$

[1] They are still objected to colour confinement, thus only quasifree.

| Symmetry | Transformation | Noether Current | Name |
|---|---|---|---|
| $SU_V(2)$ | $\psi \to e^{-i\vec{\tau}\vec{\omega}}\psi$ | $J^k_\mu = \overline{\psi}\gamma_\mu\tau^k\psi$ | isospin |
| $U_V(1)$ | $\psi \to e^{-i\alpha}\psi$ | $j_\mu = \overline{\psi}\gamma_\mu\psi$ | baryonic |
| $SU_A(2)$ | $\psi \to e^{-i\vec{\tau}\vec{\theta}\gamma_5}\psi$ | $J^k_{5\mu} = \overline{\psi}\gamma_\mu\gamma_5\tau^k\psi$ | chiral |
| $U_A(1)$ | $\psi \to e^{-i\beta\gamma_5}\psi$ | $j_{5\mu} = \overline{\psi}\gamma_\mu\gamma_5\psi$ | axial |

**Table 2.1:** Flavour space symmetries of $\mathscr{L}_{\text{chiral}}$ for two flavours with associated transformations and currents [5]. The parameters $\alpha \in \mathbb{R}$, $\beta \in \mathbb{R}$, $\vec{\omega} \in \mathbb{R}^3$ and $\vec{\theta} \in \mathbb{R}^3$ can be chosen arbitrarily.

The overall continuous symmetry group which $\mathscr{L}_{\text{chiral}}$ obeys can be written as $\mathscr{S}_{\text{QCD}} = SU_V(2) \otimes SU_A(2) \otimes U_V(1)$. It may be noted that this symmetry is only approximately satisfied by $\mathscr{L}_{\text{QCD}}$ in the case of small and similar masses. In the chiral limit ($\forall f\colon m_f = 0$), which yields $\mathscr{L}_{\text{chiral}}$, this symmetry however becomes exact. It might also be noted that the local $SU(3)_C$ group in colour space is always exact. A complete list of all flavour space symmetries can be found in Tbl. 2.1, where the shorthand notation $\psi = (q_u, q_d)^T$ is used. We discuss these symmetries now in the context of the QCD-Lagrangian $\mathscr{L}_{\text{QCD}}$, neglecting the remaining quark contributions from $\mathscr{L}_{\text{scbt}}$. $SU_V(2)$ is an approximate symmetry under the assumption $m_u \approx m_d$ and gives rise to isospin conservation. $U_V(1)$ is an exact symmetry and gives rise to baryon number conservation. $SU_A(2)$ is the chiral symmetry which is however broken for non-vanishing masses and is spontaneously broken in the ground state. The symmetry breaking can be associated with a Goldstone boson, which in this case is the pion. The $U_A(1)$ group is a symmetry in the classical sense, however is not realized in $\mathscr{S}_{\text{QCD}}$ due to quantum effects.

## 2.2 QCD matter and the phase diagram

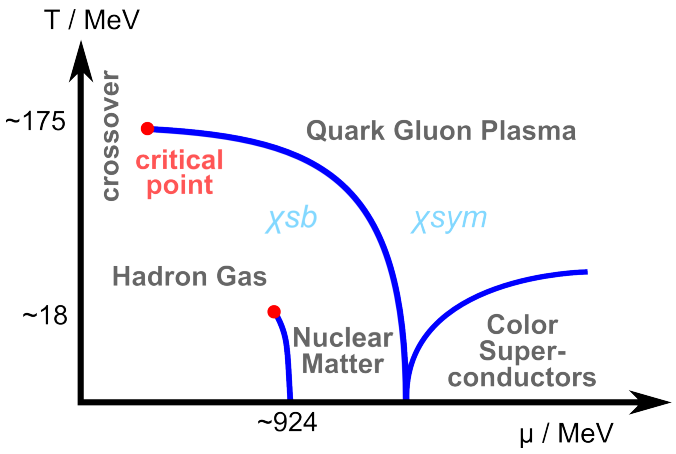


**Figure 2.1:** The QCD phase diagram as can be conjectured. Roughly based on Ref. [12].

A great research interest lies in the study of QCD matter. In this state of matter quarks and gluons are the essential degrees of freedom. Studying the thermodynamic properties for variable temperature and baryon chemical potential on the $T$-$\mu$ plane, one finds in theoretical studies that QCD matter undergoes transitions into various different phases. The visual representation of these phases is contained in the QCD phase diagram. The structure of the phase diagram pretty much depends upon the used premises and the underlying models used for description. In the following we will briefly describe the phase diagram shown in Fig. 2.1, which can be conjectured for the case of massive three flavours. Other possible phase diagrams will show behaviours which are akin to that.

At low values of $T$ and $\mu$ we find the quarks to be confined into a hadron gas. If we move along the $T$-axis for $\mu = 0$ towards higher temperatures we find a crossover transition at $T \approx 150$ - $200$ MeV, which extends to some degree into the $T$-$\mu$ plane for non-vanishing $\mu$. Moving along the $\mu$-axis we find a first-order gas-to-liquid transition into nuclear matter at $\mu \approx 924$ MeV. The phase transition extends into the $T$-$\mu$ plane until it ends in a second-order critical point at about $T \approx 15$ - $20$ MeV. Moving away further from the origin along the $\mu$-axis we find a first-order phase transition from the chirally broken ($\chi$sb) to the chirally symmetric ($\chi$sym) phase, which extends into the $T$-$\mu$ plane until it

ends in a second-order critical point, which also is a boundary of the crossover region. For high temperatures the hadron gas makes a phase transition into a quark gluon plasma via the first-order or the crossover transition. For low $T$ and large $\mu$ one finds a phase transtition to a colour superconducting phase.

As previously stated the phase diagram described above is conjectured, thus some of the proposed properties might be falsified in future studies. A more extensive and speculative description of a phase diagram can be found in Ref. [12]. Compiling a phase diagram heavily relies on the use of QCD-like theories. Although the lattice QCD approach corresponds to solving the QCD-Lagrangian numerically via Monte Carlo methods, such first principle calculations become unusable for $Re(\mu) \neq 0$ due to the fermion sign problem. For that reason several approaches are being made to circumvent this problem, ranging from extrapolations from imaginary chemical potential to various reweighting methods. One method which will play a crucial role in this work is the Taylor expansion of observables in terms of $\mu/T$. A brief discussion of the fermion sign problem and various methods can be found in Ref. [2] and [1]. However it must be noted that despite all efforts, lattice QCD calculations can only be extended to the vicinity of $\mu < T$. Thus, as long as the fermion sign problem cannot be fully resolved, lattice QCD calculations are still rendered useless for a large chunk of the $T$-$\mu$ plane.

## 2.3 The NJL model

As previously stated one way to study QCD matter is to use field theories which have a similar behaviour to the QCD-Lagrangian. Such an approach is the Nambu-Jona-Lasinio model. The Nambu-Jona-Lasinio model was originally proposed in a paper published in 1961 by Yoichiro Nambu and Giovanni Jona-Lasinio [3, 4]. Its original purpose was to describe the mass of nucleons by a process of dynamic mass generation through self-energy contributions.

The whole description is an analogy to the BCS theory of superconductivity [13], in which phonons mediate an attractive force between pairs of electrons (Cooper pairs). To create excited electron states in the superconductor one is forced to break up the Cooper pairs first, thus there is an energy gap between the ground state and excited states in the spectrum of superconductors. In the NJL model as originally proposed, the Cooper pairs have to be replaced with nucleons and anti-nucleons paired by an attractive force [3]. In this framework the nucleon masses are a consequence of this attractive interaction. Thus one speaks in the NJL model of a mass gap. Now in order to understand the QCD phase diagram, this model was later reinterpreted as a model of interacting quarks. In the same manner as before, attractive interactions now pair up quarks and anti-quarks. We additionally consider the quarks to possess a bare mass which we will denote with $m$.

Basis for this reinterpretation of the NJL model is the underlying $\mathscr{S}_{\text{NJL}} = \text{SU}_V(2)\otimes\text{SU}_A(2)\otimes\text{U}_V(1)$ symmetry in the chiral NJL-Lagrangian, which is identical to the symmetry of the chiral QCD-Lagrangian contained in $\mathscr{S}_{\text{QCD}}$. The chiral and full Lagrangian of the NJL model are given by:

$$\begin{aligned} \mathscr{L}_{\text{chiral}} &= \overline{\psi} i\partial\!\!\!/ \psi + G_S[(\overline{\psi}\psi)^2 + (\overline{\psi} i\gamma_5 \vec{\tau}\psi)^2], \\ \mathscr{L}_{\text{NJL}} &= \overline{\psi}(i\partial\!\!\!/ - \underline{m})\psi + G_S[(\overline{\psi}\psi)^2 + (\overline{\psi} i\gamma_5 \vec{\tau}\psi)^2]. \end{aligned} \tag{2.4}$$

$G_S$ denotes the interaction strength of the scalar interaction terms. If we now compare the Lagrangian of the NJL model (2.4) to the one of QCD (2.1), we see that the basic difference lies in the fact that we replaced the parts incorporating the gluon fields with mathemically much easier to handle scalar interaction terms, which still display the important symmetries. A direct consequence of these simplifications is that the $\text{SU}(3)_C$ group in colour space is now global. The chiral $\text{SU}_A(2)$ symmetry for $m = 0$ and its breaking is often coined as the most important feature of the NJL model, allowing one to investigate the chiral phase transition and its critical end point. The new interaction terms we incorporated can in fact be given a physical meaning via the *Bethe-Salpeter equation*. We can associate the first interaction term $(\overline{\psi}\psi)^2$ with a $\sigma$ meson and the second term $(\overline{\psi} i\gamma_5 \tau\psi)^2$ with a $\pi$ meson [5]. The NJL-Lagrangian as given by Eq. (2.4) can be further extended by terms which obey the symmetry $\mathscr{S}_{\text{NJL}}$. In the following we will work with a Lagrangian which is further extended by a repulsive vector interaction term [14]:

$$\mathscr{L}_{\text{NJL}} \equiv \overline{\psi}(i\partial\!\!\!/ - \underline{m})\psi + G_S[(\overline{\psi}\psi)^2 + (\overline{\psi} i\gamma_5 \vec{\tau}\psi)^2] - G_V(\overline{\psi}\gamma^\mu\psi)^2. \tag{2.5}$$

The inclusion of this term is motivated by the Walecka model, in which additionally $\omega$ mesons play an important role.

The NJL model has two great shortcomings. One being that it does not feature confinement. The other is that since the interaction terms are constructed as contact interactions, the model is nonrenormalizable. The practical consequence is that we need to define an energy scale on which the theory is valid. So in order to handle divergent momentum

integrals we must introduce a regularization scheme. Common regularization schemes are the *three-momentum cutoff*, the *four-momentum cutoff*, *regularization in proper time* and the *Pauli-Villars method*, with the latter three having the advantage of being Lorentz-invariant. In this work we will focus on the use of a three-momentum cutoff. Details on the other regularization schemes can be found in Ref. [5]. The three-momentum cutoff basically works by substituting any divergent 3d momentum integrals over the spherical domain $S_r$ with radius $r \equiv \infty$ with integrals over a spherical domain with finite radius $r \equiv \Lambda$.

In order to yield physically consistent results the cutoff parameter $\Lambda$ is of course not chosen arbitrarily. Further, the interaction strength $G_S$ and bare masses $m_f$ must also be determined in a way which yields physical meaningful results. This is usually done by fitting them to the pion mass $m_\pi$, the pion decay constant $f_\pi$ (from $\pi^- \to \mu^- + \overline{\nu}_\mu$) and the quark condensates $\langle \overline{q}_f q_f \rangle$. In this work we will assume that $m_u = m_d \equiv m$ and use a parameter set determined in Ref. [14], with $\Lambda = 587.9$ MeV, $G_S = 2.44/\Lambda^2$ and $m = 5.6$ MeV. This set is tuned to reproduce a pion mass of $m_\pi = 135$ MeV, a decay constant of $f_\pi = 92.4$ MeV and quark condensate of $\langle \overline{q}_u q_u \rangle = \langle \overline{q}_d q_d \rangle = (-240.8 \text{ MeV})^3$.

## 3 Calculations

Based on our basic understanding of the NJL model from the previous chapter, we now want to derive and motivate the introduction of the thermodynamic apparatus to describe QCD matter. In particular we are interested in calculating the grand canonical potential $\Omega$. As has been stated previously, a common technique to circumvent the fermion sign problem in lattice QCD is to expand thermodynamic functions and observables in terms of $\mu/T$. Although the NJL model is a completely different approach to describe QCD matter we will equivalently investigate an expansion in this model and compare them to results obtained in lattice QCD. In particular we are interested into whether or not the vector coupling constant $G_V$ can be tuned to deliver results which better resemble those of lattice QCD.

### 3.1 Pure scalar interaction in mean-field approximation

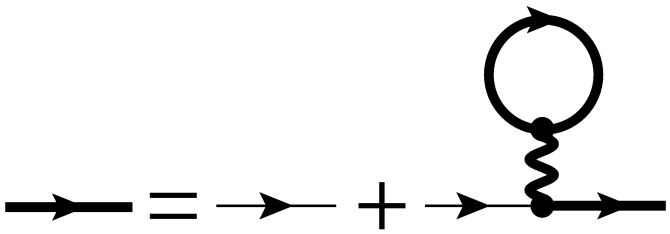

**Figure 3.1:** The Hartree approximation.

Although the bulk of this work will focus upon the inclusion of the vector interaction ($G_V \neq 0$), there is a quite demonstrative way of deriving the mass gap equation for a pure scalar interaction ($G_V = 0$) in vacuum. In particular, incorporating the vector interaction would not change it. We can obtain the mentioned equation using the Hartree approximation (see Fig. 3.1), which expresses a relationship between the propagation of quarks with a dressed mass $M$ and quarks with a bare mass $m$, where the former is denoted by thick and the latter by thin lines. In terms of operators Fig. 3.1 reads:

$$iS(p) = iS_0(p) + iS_0(p)(-i\Sigma)iS(p), \tag{3.1}$$

where $S(p)$ denotes the dressed, $S_0(p)$ the bare Feynman propagator and $\Sigma$ the self-energy contribution. The propagators are simply fermionic propagators with their respective masses. The calculation of the self-energy part is non-trivial and needs to be done explicitly for the given interaction terms. In the following we will just write down the necessary definitions and calculate $\Sigma$ straightforwardly. For a more elaborate description of the necessary Feynman rules required for the evaluation see Ref. [15]. The self-energy contribution can be calculated from the definition as follows:

$$\begin{aligned}
\Sigma &= 2iG_j\Gamma_j \int \frac{d^4k}{(2\pi)^4}\mathrm{Tr}[\Gamma_j S(k)] \\
&= 2iG_S\mathbb{1}\int \frac{d^4k}{(2\pi)^4}\mathrm{Tr}[\mathbb{1}S(k)] + 2iG_S(i\gamma_5\tau_a)\int \frac{d^4k}{(2\pi)^4}\underbrace{\mathrm{Tr}[i\gamma_5\tau_a S(k)]}_{=0} \\
&= 2iG_S\int \frac{d^4k}{(2\pi)^4}\frac{1}{k^2-M^2+i\epsilon}\mathrm{Tr}(\gamma^\mu k_\mu + M) \\
&= 2iG_S\int \frac{d^4k}{(2\pi)^4}\frac{1}{k^2-M^2+i\epsilon}N_cN_f 4M =: 8G_SN_cN_fMI(M),
\end{aligned} \tag{3.2}$$

where we have introduced the operators $\Gamma_j$ (i.e. $\Gamma_\sigma = \mathbb{1}$, $\Gamma_\pi^a = i\gamma_5\tau_a$) and the coupling constants with $G_j$ (i.e. $G_\sigma = G_\pi^a = G_S$). We implicitly assumed that operators and traces have to be evaluated on the product Hilbert space. Using these results we can now obtain the mass gap equation. Multiplying Eq. (3.1) by $S_0^{-1}(p) = \not{p} - m$ from the left side and $S^{-1}(p) = \not{p} - M$ from the right side yields:

$$\begin{aligned}
&S_0^{-1}(p) = S^{-1}(p) + \Sigma \\
\Longleftrightarrow\ &\not{p} - m = \not{p} - M + 8G_SN_cN_fMI(M) \\
\Longleftrightarrow\ &M = m + 8G_SN_cN_fMI(M).
\end{aligned} \tag{3.3}$$

The equation obtained in the last step is the mass gap equation. In particular calculating dressed masses $M$ relies on knowing the result of $I(M)$. This expression can be easily evaluated in the vacuum case using the residue theorem. However in order to introduce temperatures $T$ and chemical potential $\mu$ the $I(M)$ function has to be modified using the Matsubara formalism. The calculation could be roughly sketched in a few steps for this particular integral, but the results one obtains are the same as when choosing a more generalized approach for $G_V \neq 0$ and then setting $G_V$ a posteriori to 0. Thus we instead postpone the results for $G_V = 0$ to the latter sections of this work for a more comparative analysis and refer to [16] for an explicit treatment of the integral function $I(M)$. The important lesson of this derivation becomes clearer in the next section. To make a long story short: We will see that the case of pure scalar interaction in Hartree approximation is equivalent to the introduction of the chiral quark condensate $\langle\overline{\psi}\psi\rangle$.

### 3.2 Deriving the thermodynamic potential

We now want to calculate the thermodynamic potential $\Omega$. We start by the definition of the thermodynamic potential $\Omega$ and the partition function $Z$:

$$\begin{aligned} \Omega(T,\mu) &= -\frac{T}{V}\ln[Z(T,\mu)], \\ Z(T,\mu) &= \mathrm{Tr}[e^{-\frac{1}{T}(H-\mu N)}]. \end{aligned} \tag{3.4}$$

It has to be noted that the Hamilton function is given by $H = \int d^3x\, \mathscr{H}$ and the quark number by $N = \int d^3x\, \psi^\dagger\psi$. In this sense we calculate the Hamiltonian $\mathscr{H}$ by taking the Legendre transform of the Lagrangian $\mathscr{L}$. We further introduce the condensates $\sigma$ and $\omega$:

$$\begin{aligned} \sigma &= \langle\overline{\psi}\psi\rangle, \\ \omega &= \langle\overline{\psi}\gamma^0\psi\rangle. \end{aligned} \tag{3.5}$$

We further assume that we can approximate the interaction terms using their associated condensates, which yield $\overline{\psi}\psi = \sigma + \delta(\overline{\psi}\psi)$ and $\overline{\psi}\gamma^0\psi = \omega + \epsilon(\overline{\psi}\psi)$. We linearize the squares of the interaction terms by considering the quadratic orders of $\delta$ and $\epsilon$ as negligible. Thus we get:

$$\begin{aligned} (\overline{\psi}\psi)^2 &\approx 2\sigma(\overline{\psi}\psi) - \sigma^2 \text{ and} \\ (\overline{\psi}\gamma^0\psi)^2 &\approx 2\omega(\overline{\psi}\gamma^0\psi) - \omega^2. \end{aligned} \tag{3.6}$$

Having introduced two condensates for two interaction terms, we assume that the remaining terms do not result in condensates, thus are to be neglected [14]. This allows us to approximate the Lagrangian (2.5):

$$\begin{aligned} \mathscr{L}_{NJL} + \mu(\overline{\psi}\gamma^0\psi) &\approx \overline{\psi}(i\partial\!\!\!/ - \underbrace{(m - 2G_S\sigma)}_{=:M})\psi - \sigma^2 G_S + \omega^2 G_V + \underbrace{(\mu - 2G_V\omega)}_{=:\tilde{\mu}}\overline{\psi}\gamma^0\psi \\ &= \overline{\psi}(i\partial\!\!\!/ - M)\psi - \frac{(M-m)^2}{4G_S} + \frac{(\mu-\tilde{\mu})^2}{4G_V} + \tilde{\mu}\,\psi^\dagger\psi =: \mathscr{L} + \mu\,\psi^\dagger\psi. \end{aligned} \tag{3.7}$$

We have introduced the dressed quark mass $M$ and the renormalized chemical potential $\tilde{\mu}$ via gap equations:

$$\begin{aligned} M &= m - 2G_S\sigma, \\ \tilde{\mu} &= \mu - 2G_V\omega. \end{aligned} \tag{3.8}$$

In particular getting solutions for $M$ and $\tilde{\mu}$ requires one to calculate $\sigma$ and $\omega$ first (which are again functions of $M$ and $\tilde{\mu}$) and then to solve the gap equations self-consistently. The condensates can be calculated straightforwardly from the definition of the thermal expectation values and subsequent application of the Matsubara formalism or as a consequence by enforcing thermodynamic consistency. We will choose the latter approach, however set aside an explicit discussion for the next section. Taking the Legendre transform, we obtain:

$$\mathscr{H} = \dot{\psi}^{(j)}\pi^{(j)} - \mathscr{L} = -\overline{\psi}(i\gamma^k\partial_k - M)\psi + \frac{(M-m)^2}{4G_S} - \frac{(\mu-\tilde{\mu})^2}{4G_V} - (\tilde{\mu}-\mu)\psi^\dagger\psi, \tag{3.9}$$

with $j$ denoting the components of the Dirac spinor, $\pi$ the field momentum and $k$ the spatial components. Putting the result into Eq. (3.4), we see that $\Omega$ decomposes into a non-trivial and a trivial part:

$$\Omega(T,\mu;M,\tilde{\mu}) = \underbrace{-\frac{T}{V}\ln\{\mathrm{Tr}[\exp\left(-\frac{1}{T}\int d^3x\, -\overline{\psi}(i\gamma^k\partial_k - M)\psi - \tilde{\mu}\,\psi^\dagger\psi\right)]\}}_{\text{non-trivial}} + \underbrace{\frac{(M-m)^2}{4G_S} - \frac{(\mu-\tilde{\mu})^2}{4G_V}}_{\text{trivial}}. \tag{3.10}$$

Note: $M$ and $\tilde{\mu}$ are no independent variables but functions of $\mu$ and $T$. Thus we seperated them in the function header. Let us take a further look and identify some of the terms in the non-trivial part which we will denote with $\Omega_M$:

$$\Omega_M(T,\mu;M,\tilde{\mu}) = -\frac{T}{V}\ln\{\mathrm{Tr}[\exp\left(-\frac{1}{T}\int d^3x\, \underbrace{-\overline{\psi}(i\gamma^k\partial_k - M)\psi}_{\mathscr{H}_{\text{free}}} - \tilde{\mu}\,\underbrace{\psi^\dagger\psi}_{\mathscr{N}}\right)]\} = -\frac{T}{V}\ln(Z_{\text{free}}). \tag{3.11}$$

The argument of the potential is resembling to a free Fermi gas with mass $M$ and chemical potential $\tilde{\mu}$. An explicit calculation of that expression is possible but lengthy and is given in Ref. [17] for a flavour- and colourless gas ($N_c$= $N_f$=1) of fermions and anti-fermions. In the following we will just give the final result of $\ln(Z_{\text{free}})$ and explain the physical meaning of the terms.

$$\ln(Z_{\text{free}}) = \underbrace{2N_cN_f}_{\substack{\text{spins, colours}\\ \text{and flavours}}} V \int \frac{d^3p}{(2\pi)^3}\left\{\underbrace{\frac{E_p}{T}}_{\substack{\text{zero-point}\\ \text{energy}}} + \underbrace{\ln[1+\exp\left(-\frac{1}{T}(E_p-\tilde{\mu})\right)]}_{\text{quark contribution}} + \underbrace{\ln[1+\exp\left(-\frac{1}{T}(E_p+\tilde{\mu})\right)]}_{\text{anti-quark contribution}}\right\}. \tag{3.12}$$

The prefactor $2N_cN_f$ is the result of up and down spins, as well as the colours and flavours. The integral over the zero-point energy term $E_p/T$ is divergent and needs to be treated by a regularization scheme of choice (in our case the three-momentum cutoff). The remaining terms are contributions from quarks and anti-quarks. For the sake of completeness we will now write down the final result for the thermodynamic potential $\Omega$:

$$\begin{aligned}\Omega(T,\mu;M,\tilde{\mu}) = {} & \frac{(M-m)^2}{4G_S} - \frac{(\mu-\tilde{\mu})^2}{4G_V} \\ & - 2N_cN_f\left\{\int_{S_\Lambda}\frac{d^3p}{(2\pi)^3}E_p + \int_{\mathbb{R}^3}\frac{d^3p}{(2\pi)^3}\left[T\ln(1+\mathrm{e}^{-\frac{1}{T}(E_p-\tilde{\mu})}) + T\ln(1+\mathrm{e}^{-\frac{1}{T}(E_p+\tilde{\mu})})\right]\right\}.\end{aligned} \tag{3.13}$$

### 3.3 Self-consistency equations

As previously stated the equations (3.8) define us a set of gap equations which needs to be self-consistently solved. As a first step one needs to calculate explicit expressions for the condensates $\sigma = \sigma(T,\mu;M,\tilde{\mu})$ and $\omega = \omega(T,\mu;M,\tilde{\mu})$. For a thermodynamic consistent treatment we require that [14]:

$$\frac{d\Omega}{dm} \overset{!}{=} \frac{\partial\Omega}{\partial m} = \sigma \quad \text{and} \quad -\frac{d\Omega}{d\mu} \overset{!}{=} -\frac{\partial\Omega}{\partial\mu} = \omega. \tag{3.14}$$

Calculating the total derivatives, we find that the partial derivatives $\partial_M\Omega$ and $\partial_{\tilde{\mu}}\Omega$ have to vanish in order to meet the previously mentioned requirements. This leads to a set of equations which gives us explicit expressions for the condensates $\sigma$ and $\omega$:

$$\begin{aligned}0 = \frac{\partial\Omega}{\partial M} &= \frac{M-m}{2G_S} - 2N_fN_c\int\frac{d^3p}{(2\pi)^3}\frac{M}{E_p}[1-n_p(T,\tilde{\mu})-\overline{n}_p(T,\tilde{\mu})] = \frac{M-m}{2G_S} + \sigma, \\ 0 = \frac{\partial\Omega}{\partial\tilde{\mu}} &= \frac{\mu-\tilde{\mu}}{2G_V} - 2N_fN_c\int\frac{d^3p}{(2\pi)^3}[n_p(T,\tilde{\mu})-\overline{n}_p(T,\tilde{\mu})] = \frac{\mu-\tilde{\mu}}{2G_V} - \omega.\end{aligned} \tag{3.15}$$

We have introduced the quark occupation number

$$n_p(T,\tilde{\mu}) = \frac{1}{1+\exp[-1/T(E_p-\tilde{\mu})]} \tag{3.16}$$

and anti-quark occupation number $\overline{n}_p(T,\tilde{\mu}) = n_p(T,-\tilde{\mu})$. One can interpret the equations (3.15) in terms of vector calculus: Arbitrary points $(M,\tilde{\mu})$ at a preset temperature $T$ and chemical potential $\mu$ are only solutions if they form extrema of $\Omega$. A problem which becomes evident is that the map $(T,\mu)\to(M,\tilde{\mu})$ is not necessarily injective, thus we may find more than one solution for a given point $(T,\mu)$. Since in thermodynamics the potential $\Omega$ is supossed to be minimized, we will assume that the physically valid solution $(M,\tilde{\mu})$ is the one which minimizes $\Omega$ the most. The solution of the equation for $\tilde{\mu}$ is always unique for a given point $(T,\mu,M)$. At constant $T$ and $\mu$ this allows us to introduce the parameterization $\tilde{\mu} = \tilde{\mu}(M)$ and $\Omega(M) = \Omega(M,\tilde{\mu}(M))$. So finding the physically legitimate solution $(M,\tilde{\mu}(M))$ now only corresponds to finding the global minimum of $\Omega(M)$.

## 3.4 Extrema of the thermodynamic potential

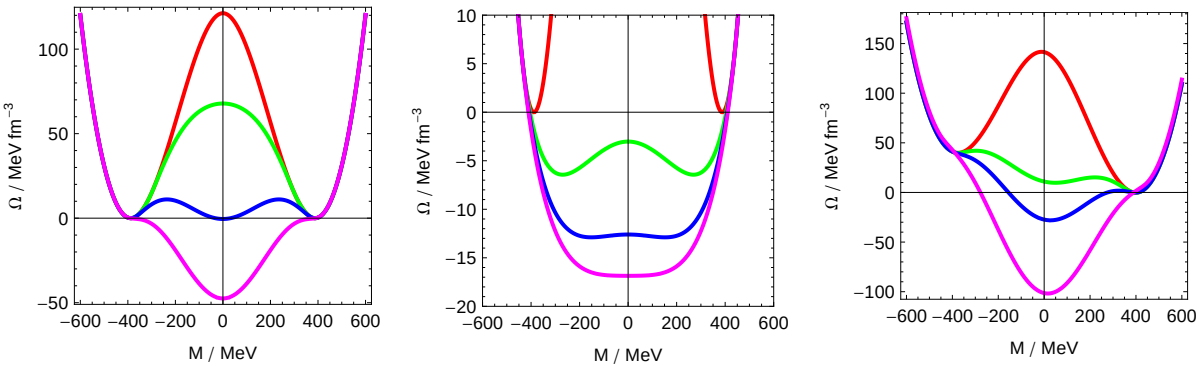


**Figure 3.2:** Plots of the thermodynamic potential $\Omega(M)$ for different constant $\mu$.
Left image: $G_V = 0$, $m = 0$; $\mu = 0, 300, 368.6$ and 400 MeV (red, green, blue, magenta).
Middle image: $G_V = G_S$, $m = 0$; $\mu = 0, 430, 440$ and 444.3 MeV (red, green, blue, magenta).
Right image: $G_V = 0$, $m = 5.6$ MeV; $\mu = 0, 375, 400$ and 440 MeV (red, green, blue, magenta).

In this section we will discuss the influence of the bare mass $m$ and the vector coupling constant $G_V$ on the extrema of $\Omega(M)$, which we know from the previous section are essential for knowing the legitimate solutions $(M, \tilde{\mu}(M))$ for a given point $(T, \mu)$. In this section we set $T = 1$ MeV and investigate the behaviour of $\Omega(\mu; M, \tilde{\mu}(\mu, M))$ on the $\mu$-$M$ plane.

In Fig. 3.2 are three plots of the thermodynamic potential in the range from $\mu = 0$ to 444.3 MeV. The specific values for $\mu$ used in the plots were chosen to make characteristic behaviour evident, thus the plots are not directly comparable. In the first and the second plot the bare mass $m$ is kept constant at $m = 0$ (chiral limit) and the coupling constant $G_V$ is varied from 0 (first plot) to $G_S$ (second plot). The thermodynamic potential $\Omega$ remains symmetric, which is an obvious behaviour when considering the mass gap equation under the sign transformation $M \to -M$ in the chiral limit. The characteristic features however change significantly. Although we observe a characteristic $\mu$ for $G_V = 0$ at which the mass gap equation has five numerical solutions, we find that such a value of $\mu$ does not exist for $G_V = G_S$, at which the mass gap equation yields at maximum only three numerical solutions. An interesting feature is that although one can easily verify that the mass gap equation always yields the trivial solution $M = 0$ in the chiral limit, this solution is not the physically relevant one for too low values of $\mu$, even forming a maximum for low enough values. Another consequence of the symmetry is that for low values of $\mu$ one observes two identical solutions $|M|$ with different algebraic sign. These can however not be distinguished by the minimization criteria. We therefore will just assume that the physical mass can only be positive.

Abandoning the discussion of the influence of the coupling constant $G_V$, we now investigate the influence of the bare mass $m$ on the thermodynamic potential. In the first and the third plot of Fig. 3.2 the coupling constant $G_V$ is kept constant at $G_V = 0$ and we vary the bare mass $m$ from $m = 0$ (first plot) to 5.6 MeV (third plot). While one can see that $\Omega$ keeps its general shape, one can also see that the plot is skewed compared to the chiral limit. The main consequence of this is that the trivial solution $M = 0$ disappears and is replaced by solutions of $M \gtrsim 0$. The general trend which can be observed in all plots, is that for large $\mu$ there is only one numerical solution which either is $M = 0$ (chiral limit) or $m \gtrsim M$. This behaviour is somewhat intuitive when considering that our model reflects the chiral phase transition in the QCD phase diagram and therefore tries to replicate the bare quark mass $m$. Deviations from this expected behaviour can be dependent on the used regularization scheme.

## 3.5 Solutions of the self-consistency equations for variable chemical potential

In pursuit of automating the sketched way of solving $M$ for variable $\mu$ in the previous section (we keep the temperature at $T = 1$ MeV), we can construct an algorithm which is capable of providing a function $M(\mu)$. The resulting plots for variable coupling constant $G_V$ and bare mass $m$ are listed in the upper row of Fig. 3.3.
We can observe that the generated dynamical mass $M$ is discontinuous in $\mu$ for $G_V = 0$ and $0.5\,G_S$, whereas it is continuous for $G_V = G_S$. The discontinuous behaviour is already evident when comparing the parametric plots of the

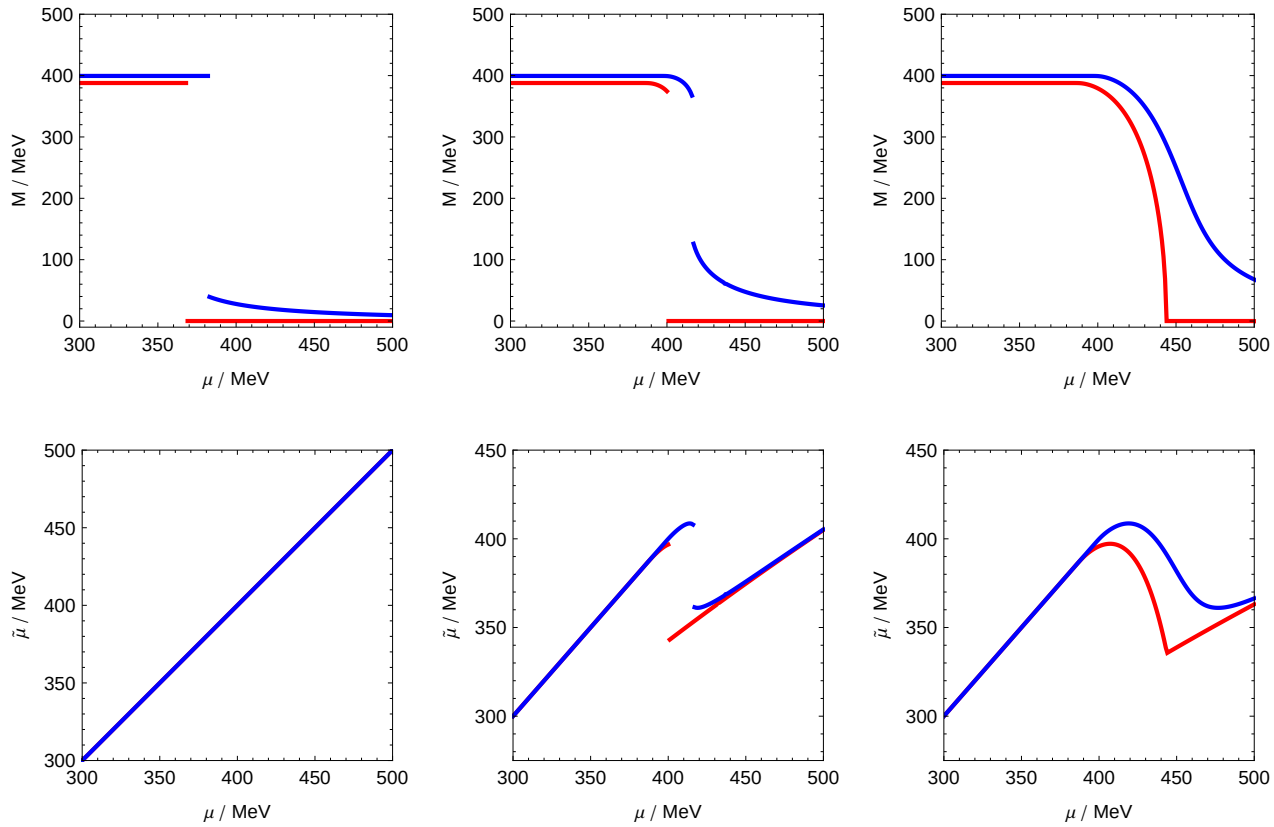


**Figure 3.3:** Plots of $M(\mu)$ (upper row) and $\tilde{\mu}$ (lower row) for variable bare quark mass $m$ and vector coupling constant $G_V$. From left to right: $G_V = 0$, $0.5\,G_S$ and $G_S$. The blue lines correspond to $m = 5.6$ MeV and the red lines to $m = 0$.

thermodynamic potential in Fig. 3.2. The plots in Fig. 3.3 can already be used to classify phase transitions. The discontinuous behaviours of the mass plots for $G_V = 0$ and $G_V = 0.5\,G_S$ are classified as first order phase transitions. In particulary they correspond to the chiral phase transition at $T = 1$ MeV in the phase diagram in Fig. 2.1. The phase transition for $G_V = G_S$ and $m = 0$ is continuous, however it is discontinuous in its derivative with respect to $\mu$. This is classified as second order phase transition. The case of $G_V = G_S$ and $m = 5.6$ MeV is continuous in all of its derivatives with respect to $\mu$. It is commonly labeled as a crossover transition, however, in fact it is not a phase transition.

Since we now have a function $M(\mu)$ we can also calculate solutions $\tilde{\mu}(\mu) = \tilde{\mu}(\mu, M(\mu))$. The resulting plots are given in the lower row of Fig. 3.3. The $G_V = 0$ case is obvious since the second gap equation yields $\tilde{\mu} = \mu$, the course of the remaining plots for $G_V = 0.5$ and $G_S$ is a direct consequence of the behaviour of $M(\mu)$, thus will not be further discussed.

## 3.6 Calculation of the Taylor coefficients to sixth order

We now want to calculate the Taylor coefficients of the thermodynamic potential $\Omega(T, \mu)$ in terms of $\mu/T$ at the expansion point $\mu/T = 0$ to sixth order. We therefore just expand $\Omega$ in terms of $\mu/T$:

$$\Omega(T,\mu) = \sum_{n=0}^{\infty} c_n^* \left(\frac{\mu}{T}\right)^n = \sum_{n=0}^{\infty} \frac{1}{n!} \frac{\partial^n \Omega}{\partial (\mu/T)^n}\bigg|_{\mu/T=0} \left(\frac{\mu}{T}\right)^n . \tag{3.17}$$

Further we will follow the convention of using the reduced thermodynamic potential $\tilde{\Omega} = -\Omega/T^4$, thus effectively multiplying the definition of the coefficient by a prefactor:

$$c_n = -\frac{1}{T^4} c_n^* = -T^{n-4} \frac{1}{n!} \frac{\partial^n \Omega}{\partial \mu^n}\bigg|_{\mu=0} . \tag{3.18}$$

We can calculate the Taylor coefficients from the definition (3.18) straightforwardly. However, we only have to calculate the Taylor coefficients of even order. This property is realized due to the symmetry of $\Omega$ under charge conjugation, which is a fundamental property of QCD. In a world in which we replace quarks by anti-quarks and vice versa the physics should stay the same. We can further prove that this property is fulfilled using the gap equations (3.15).

Using the gap equation of the renormalized chemical potential $\tilde{\mu}$ and the fact that solutions of this equation are unique for a given point $(T,\mu,M)$, we find under the transformation $\mu \to -\mu$, that $-\tilde{\mu}(-\mu) = \tilde{\mu}(\mu)$, thus rendering the solutions anti-symmetric in $\mu$. Further taking a look at the mass gap equation shows that $M(\tilde{\mu}(\mu)) = M(-\tilde{\mu}(\mu)) = M(\tilde{\mu}(-\mu))$, thus rendering the solutions symmetric in $\mu$. So in conclusion we find that $(\tilde{\mu}, M) \xrightarrow{\mu\to-\mu} (-\tilde{\mu}, M)$. It is now quite obvious when applying the transformation to Eq. (3.13) that $\Omega$ is symmetric in $\mu$. In particular we can now easily prove that odd terms have to vanish in the Taylor expansion:

$$\Omega(T,\mu) = \sum_{n \text{ even}}^{\infty} c_n^* \left(\frac{\mu}{T}\right)^n + \sum_{n \text{ odd}}^{\infty} c_n^* \left(\frac{\mu}{T}\right)^n \overset{!}{=} \sum_{n \text{ even}}^{\infty} c_n^* \left(\frac{\mu}{T}\right)^n + \sum_{n \text{ odd}}^{\infty} -c_n^* \left(\frac{\mu}{T}\right)^n = \Omega(T,-\mu). \tag{3.19}$$

Thus Eq. (3.19) is only satisfied for non-vanishing values $\mu/T$, if odd ordered coefficients vanish □.

So we now only have to calculate the Taylor coefficients of second, fourth and sixth order. For that purpose we will use the finite difference method and approximate the derivatives with central difference quotients. In particular we use:

$$\begin{aligned}
\left.\frac{\partial^2\Omega}{\partial\mu^2}\right|_{\mu=0} &\approx \frac{1}{12\Delta^2}\Big\{2[-\Omega(2\Delta)+16\Omega(\Delta)]-30\Omega(0)\Big\},\\
\left.\frac{\partial^4\Omega}{\partial\mu^4}\right|_{\mu=0} &\approx \frac{1}{6\Delta^4}\Big\{2[-\Omega(3\Delta)+12\Omega(2\Delta)-39\Omega(\Delta)]+56\Omega(0)\Big\} \text{ and}\\
\left.\frac{\partial^6\Omega}{\partial\mu^6}\right|_{\mu=0} &\approx \frac{1}{240\Delta^6}\Big\{2[13\Omega(5\Delta)-190\Omega(4\Delta)+1305\Omega(3\Delta)-4608\Omega(2\Delta)+9690\Omega(\Delta)]-12276\Omega(0)\Big\}.
\end{aligned} \tag{3.20}$$

The expressions were shortened using the symmetry of $\Omega$ in respect to $\mu = 0$. The order of approximation was chosen so that approximation errors are of third power in $\Delta$ for the second and fourth derivative and of fifth power for the sixth derivative. This directly corresponds to using five, seven and eleven sampling points for the derivatives. Further the grid spacing was chosen for every coefficient so that numerical errors which become emergent for large values of $T$ and too small grid spacing are minimized.

When discussing the course of the Taylor coefficients in the high temperature district, it is useful to refer to the limits of the Stefan-Boltzmann gas. The Stefan-Boltzmann gas with thermodynamic potential $\Omega_{SB}$, corresponds to the potential of a free quark gluon gas:

$$-\frac{\Omega_{SB}}{T^4} = 2N_cN_f\left[\frac{7\pi^2}{360}+\frac{1}{12}\left(\frac{\mu}{T}\right)^2+\frac{1}{24\pi^2}\left(\frac{\mu}{T}\right)^4\right]-\frac{\Omega_{\text{glue}}}{T^4}, \tag{3.21}$$

where $\Omega_{\text{glue}}$ is the gluonic contribution with $\Omega_{\text{glue}} \propto T^4$. The Stefan-Boltzmann limits of the coefficients can now be straightforwardly calculated by taking the derivatives of $\Omega_{SB}$ and the limit $\mu/T \to 0$ . In particular we find in this limit: $c_2 = 1$, $c_4 = 0.051$ and $c_6 = 0$.

A presentation of all calculated Taylor coefficients for $m = 5.6$ MeV, variable order $n$ and vector coupling constant $G_V$ is given in Fig. 3.4. All calculations were performed in C++ using some functions contained in the GNU Scientific Library. Roughly, one can say that coefficients of second and fourth order are always positive, have one maximum or become asymptotical constant for $G_V = 0$ and large $T$, while sixth order coefficients always become asymptotical zero, but also possess a zero crossing, a positive maximum and a negative minimum. Much more information yields the comparison for constant order $n$ and variable coupling constant $G_V$, which we can see in the fourth lower row in Fig. 3.4. The second order coefficient at $G_V = 0$ is a steeply rising function reaching a plateau value of $c_2 \approx 1$ for large $T$. Putting in a vector interaction destroys the constant Stefan-Boltzmann limit and creates a global positive maximum at about $T \approx 200$ MeV, which becomes smaller the greater $G_V$ gets. The fourth order coefficient is also a steeply rising function, reaching a global maximum at about $T \approx 190$ MeV and then sinking to reach its Stefan-Boltzmann limit for large $T$ of about $c_4 \approx 0.051$. Turning on the vector interaction also destroys the Stefan-Boltzmann limit and results into the maximum shrinking the greater $G_V$ gets. The sixth order coefficient rises first to a positive maximum, then does a zero crossing, reaches a minimum and approaches then 0 for large $T$. Turning on the vector interaction drastically reduces the magnitudes of the extrema.

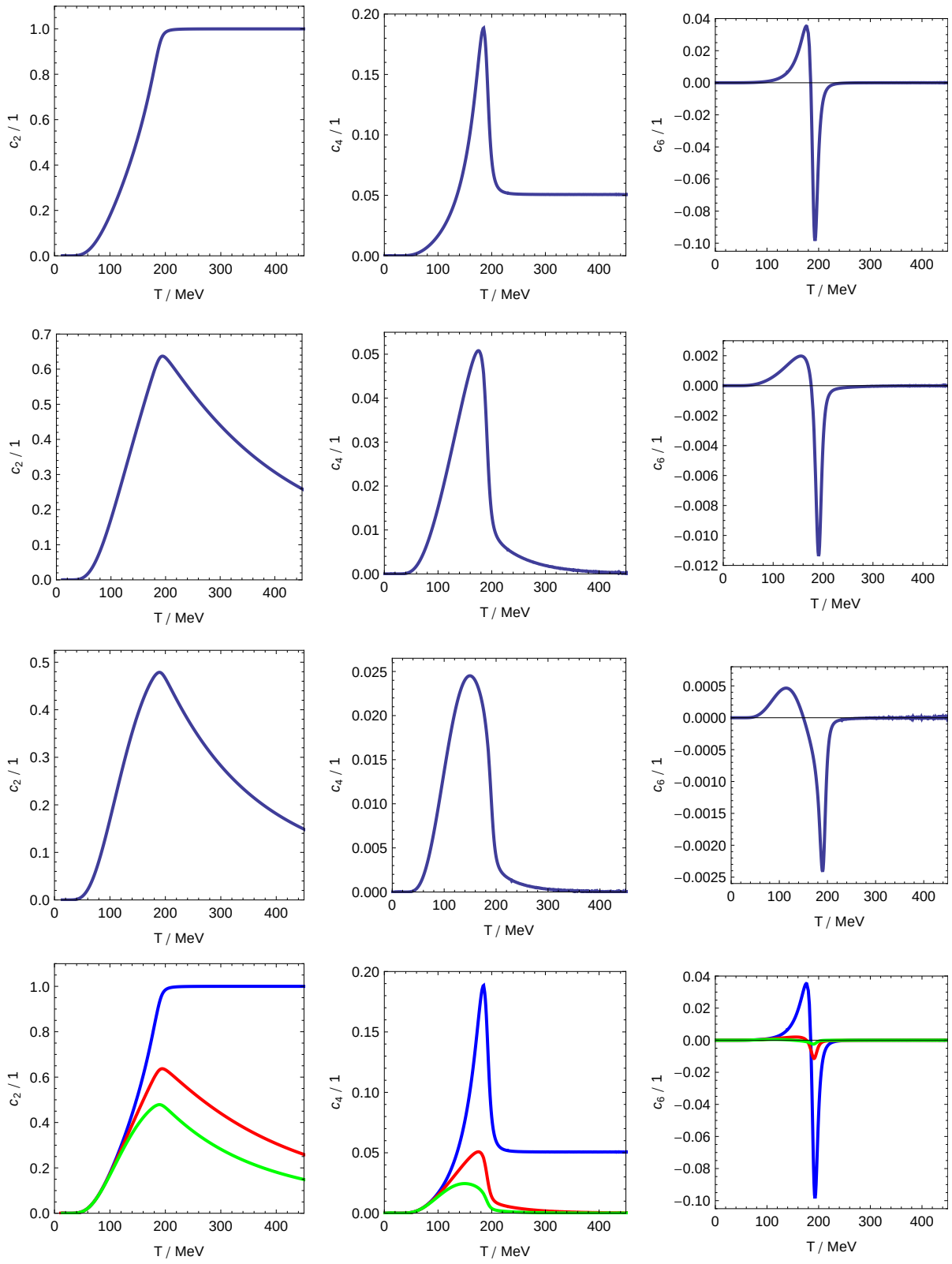


**Figure 3.4:** Taylor coefficients of variable order $n$ and vector coupling constant $G_V$.
From left to right: Taylor coefficients of order 2, 4 and 6.
First three rows from top to bottom: Taylor coefficients for $G_V = 0$, $0.5\,G_S$ and $G_S$.
Fourth row on the bottom: Comparative plots the Taylor coefficients for coupling constant $G_V = 0$, $0.5\,G_S$ and $G_S$ (blue, red, green).

## 3.7 Comparison to lattice data

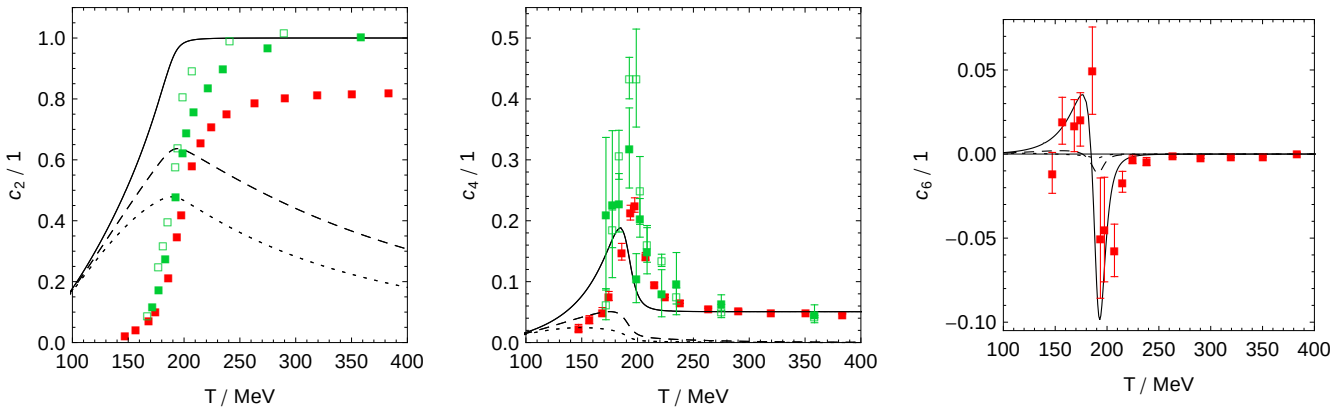


**Figure 3.5:** Comparison of Taylor coefficients $c_2$, $c_4$ and $c_6$ (left to right) obtained from lattice QCD calculations (red and green) to the vector interaction extended NJL model (black). Red squares represent data by C.R. Allton et al. [6] and green squares M. Cheng et al. [7]. Empty green squares were done on a $16^3 \times 4$ lattice, filled green squares on a $24^3 \times 6$ lattice. The vector coupling strength is set in the extended NJL model to $G_V = 0$, $0.5\,G_S$ and $G_S$ (continuous, dashed, dotted).

In this section we now want to compare the results we have obtained to available lattice data and find out whether or not we can tune the vector coupling constant $G_V$ to deliver better results with the vector interaction extended NJL model. In particular we will use results of calculations done by C.R. Allton et al. [6] (red data) for two flavours on a $16^3 \times 4$ lattice using p4-improved staggered fermions with bare quark mass $m/T = 0.4$ and M. Cheng et al. [7] (green data) for three flavours on a $16^3 \times 4$ and a $24^3 \times 6$ lattice using p4-improved staggered fermions and fixed quark masses. The data can be directly found in Ref. [6] and [7], errors were taken from the plots. The temperature values which were used for the calculated sampling points are all given in respect to the pseudocritical temperature $T_0$, which is the temperature at which the crossover transition for $\mu = 0$ is located. This allows us to translate the results into the NJL model, in which the pseudocritical temperature is estimated to be $T_0 = 193.6$ MeV [16].

Comparing the lattice data with the results in our extended NJL model (Fig. 3.5), we see that the course of the Taylor coefficients, as well as the Stefan-Boltzmann limits, are best replicated by the NJL model for $G_V = 0$. Further one finds a systematic discrepance between lattice data and the NJL model. For the lattice data of $c_2$ and $c_4$ one sees that the flank is significantly shifted to higher temperatures. For data provided by Ref. [6] (red) $c_2$ does not reach the predicted Stefan-Boltzmann limit, instead converges towards $c_2 \approx 0.8$. This does not comply with data provided by Ref. [7] (green), in which $c_2$ does indeed reach its predicted limit. So this abberation might be a result due to the temperature dependent bare mass. The remaining coefficients $c_4$ and $c_6$ seem to follow the trend of converging towards their predicted limits. A notable feature of $c_4$ in lattice calculations is that its peak is higher than in the NJL model. The data provided on $c_6$ is highly speculative due to the large errors, however for that reason complies with the scalar NJL model except for a few data points.

Overall the study confirms a similar analysis done by J. Steinheimer and S. Schramm in 2011 [18], comparing second and fourth order Taylor coefficients of the PNJL and QHC model with lattice QCD calculations from Ref. [7].

## 4 Résumé and outlook

The motivation of this work was to investigate the Taylor coefficients of the NJL model under the inclusion of a repulsive vector interaction term $-G_V(\overline{\psi}\gamma^\mu\psi)^2$ and find out whether or not the vector coupling $G_V$ can be tuned to deliver better results in comparison to lattice QCD calculations. For the investigation the NJL model in the two flavour case under the inclusion of an up and down quark of equal mass and chiral condensate was chosen. Divergent momentum integrals are regularized using a sharp three-momentum cutoff, which however is not Lorentz invariant. The parameter set which is used was determined by Ref. [14].

Investigating first the case of a pure scalar interaction, which is the special case for $G_V = 0$, actually shows that one can derive the mass gap equation using the Hartree approximation. In particular this is equivalent to the introduction of the chiral quark condensate $\langle\overline{\psi}\psi\rangle$. The Lagrangian with the vector interaction term can be treated by the introduction of the condensates $\langle\overline{\psi}\psi\rangle$ and $\langle\overline{\psi}\gamma^0\psi\rangle$. These condensates result into a set of two gap equations, one describing the generated mass $M$ and the other the renormalized chemical potential $\tilde{\mu}$. Approximating the interaction terms with their associated condensates allows us to calculate the thermodynamic potential $\Omega$ of the grand canonical ensemble. One can show that pairs of $M$ and $\tilde{\mu}$ are only valid solutions of the gap equations if they are extrema of $\Omega$. If there is more than one solution $(M, \tilde{\mu})$ for a given point $(T, \mu)$, the one is chosen which is a global minimum of $\Omega$. Following these principles one can now construct an algorithm to calculate $(M, \tilde{\mu})$ for any given point $(T, \mu)$ and thus $\Omega$. Calculating the Taylor coefficients can now be done numerically using finite differences. Furthermore one just needs to calculate even ordered coefficients. The odd orders vanish as a direct consequence of the symmetry of QCD under charge conjugation ($\mu \to -\mu$) and thus $\Omega$. In general a non-vanishing vector interaction ($G_V \neq 0$) leads to a reduction of the magnitude of the course of the coefficients. Further the Stefan-Boltzmann limits are destroyed for $c_2$ and $c_4$. Comparing the coefficients to lattice data from Ref. [6] and [7] shows that there are some significant discrepancies, however the course of the lattice results, as well as the Stefan-Boltzmann limits, are best replicated by neglecting the vector interaction term. This conclusion complies with an analysis of Taylor coefficients done in Ref. [18] for the PNJL and QHC model.

Summing up the results one obtains from the study of these QCD-like theories shows that it seems to become evident that vector interaction terms generally are negligible if one aims to get results which are similar to those of lattice QCD. Although this should hold up to various other lattice QCD extension methods apart from the Taylor expansion technique, it is an interesting afterthought whether or not the effects are as drastical. An answer to this question therefore remains open for future studies.

## Bibliography


[1] M. P. Lombardo, "Lattice QCD at finite temperature and density," *Modern Physics Letters A*, vol. 22, pp. 457–472, 2005.

[2] C. Schmidt, "Lattice QCD at finite density," *PoS*, vol. LAT2006, p. 021, 2006.

[3] Y. Nambu and G. Jona-Lasinio, "Dynamical model of elementary particles based on an analogy with superconductivity. I," *Phys. Rev.*, vol. 122, pp. 345–358, 1961.

[4] Y. Nambu and G. Jona-Lasinio, "Dynamical model of elementary particles based on an analogy with superconductivity. II," *Phys. Rev.*, vol. 124, pp. 246–254, 1961.

[5] S. P. Klevansky, "The Nambu-Jona-Lasinio model of quantum chromodynamics," *Review of Modern Physics*, vol. 64, pp. 649–708, 1992.

[6] C. R. Allton et al., "Thermodynamics of Two Flavor QCD to Sixth Order in Quark Chemical Potential," *Phys. Rev. D*, vol. 71, p. 054508, 2005.

[7] M. Cheng et al., "Baryon number, strangeness, and electric charge fluctuations in QCD at high temperature," *Phys. Rev. D*, vol. 79, p. 074505, 2009.

[8] M. Ablikim et al., "Observation of a charged charmoniumlike structure in $e^+e^- \to \pi^+\pi^- J/\psi$ at $\sqrt{s} = 4.26\,\mathrm{GeV}$," *Phys. Rev. Lett.*, vol. 110, p. 252001, 2013.

[9] Z. Q. Liu et al., "Study of $e^+e^- \to \pi^+\pi^- J/\psi$ and observation of a charged charmoniumlike state at Belle," *Phys. Rev. Lett.*, vol. 110, p. 252002, 2013.

[10] G. Ecker, "Quantum Chromodynamics," *arXiv:1205.1815*, 2006.

[11] A. Grozin, "Quantum Chromodynamics," *arXiv:hep-ph/0604165*, 2012.

[12] K. Fukushima and T. Hatsuda, "The phase diagram of dense QCD," *Rept. Prog. Phys.*, vol. 74, p. 014001, 2010.

[13] J. Bardeen, L. N. Cooper and J. R. Schrieffer, "Microscopic theory of superconductivity," *Phys. Rev.*, vol. 106, pp. 162–164, 1957.

[14] M. Buballa, "NJL-model analysis of dense quark matter," *Phys.Rept.*, vol. 407, pp. 205 – 376, 2004.

[15] S. Möller, "Pion-Pion scattering and shear viscosity in the Nambu-Jona-Lasinio model," Master's thesis, TU Darmstadt, 2013.

[16] D. Scheffler, "NJL model study of the QCD phase diagram using the taylor expansion technique," Bachelor's thesis, TU Darmstadt, 2007.

[17] J. I. Kapusta and C. Gale, *Finite-Temperature Field Theory*. Cambridge University Press, 2006.

[18] J. Steinheimer and S. Schramm, "The problem of repulsive quark interactions - Lattice versus mean field models," *Phys. Lett. B*, vol. 696, pp. 257 – 261, 2011.